Ultramicroscopy 122 (2012) 26–31

Contents lists available at SciVerse ScienceDirect

Ultramicroscopy

journal homepage: www.elsevier.com/locate/ultramic

Atomic force microscope based biomolecular force-clamp measurements using a micromachined electrostatic actuator

Hamdi Torun [a,*], Ofer Finkler [b], F. Levent Degertekin [b]

[a] Department of Electrical and Electronics Engineering, Bogazici University, Bebek, TR-34342 Istanbul, Turkey
[b] G.W. Woodruff School of Mechanical Engineering, Georgia Institute of Technology, Atlanta GA 30332, USA

ARTICLE INFO

Article history:
Received 14 December 2011
Received in revised form
18 May 2012
Accepted 17 July 2012
Available online 31 July 2012

Keywords:
Atomic force microscopy
Microsystems
Force spectroscopy
Single molecule mechanics

ABSTRACT

The authors describe a method for biomolecular force clamp measurements using atomic force microscope (AFM) cantilevers and micromachined membrane-based electrostatic actuators. The actuators comprise of Parylene membranes with embedded side actuation electrodes and are fabricated on a silicon substrate. The devices have a displacement range of 1.8 μm with 200 V actuation voltage, and displacement uncertainty is 0.8 nm, including the noise and drift. The settling time, limited by the particular amplifier is 5 ms, with an inherent range down to 20 μs. A force clamp measurement setup using these actuators in a feedback loop has been used to measure bond life-times between human IgG and anti-human IgG molecules to demonstrate the feasibility of this method for biological experiments. The experimental findings are compared with a molecular pulling experiment and the results are found to be in good agreement.

© 2012 Elsevier B.V. All rights reserved.

1. Introduction

Cell-adhesion molecules (e.g. integrins, selectins and immunoglobulins) mediate a variety of biophysical processes. Single-molecule experiments employing an atomic force microscope (AFM) can measure mechanical properties of biomolecular bonds directly to study these processes such as cell tethering [1–3], antigen binding to antibody [4,5], and protein folding/unfolding [6–9].

Conventional AFM systems use a micro-scale cantilever as a force sensor. The cantilever, coated with biomolecules is actuated against a sample surface using a piezo actuator. In an open-loop operation, the piezo pulls the cantilever away from the sample surface at a constant speed. The interaction force between the biomolecules on the cantilever and the sample surface are recorded by measuring the deflection of the cantilever. Varying the pulling speed and measuring the strength of adhesion/rupture events, kinetic off-rates associated with biological weak bonds can be determined based on a kinetic rate model also called as Bell–Evans model [10–12]. This, however, is rather an indirect way of measuring off-rates and bond life-times. Bond life-times can be measured directly when the cantilever is controlled in a feedback loop. This closed-loop mode of operation is called force-clamp spectroscopy where the force on the cantilever is kept constant by controlling the piezo actuator [6,9]. A constant force stretches the biological bond, and the time until the bond ruptures is measured as the bond life-time. Force-clamp spectroscopy measures time-domain information hence assesses life-time directly Force-clamp spectroscopy has been employed to measure biological events such as protein folding/unfolding [6,7], receptor–ligand dissociation [13] and association [14]. When used for protein unfolding measurements, faster operation allows the complete detection of unfolding patterns with high precision. Fast operation is also needed for molecular life-time measurements. This capability not only improves temporal resolution, but it also allows the measurement of short life-times, especially observed when the stretching force is higher.

Traditionally, closed-loop operation of the piezo actuator determines the dynamic performance of a force-clamp setup. Both analog [15] and software-based digital PID controllers [16,17] have been developed to optimize the operation. Typical response time of these setups is ~3–6 ms with an actuation resolution of ~0.5–1 nm. Response time of a force-clamp setup is usually limited by the speed of actuators. Unloaded resonant frequency of commercial stack piezo actuators can reach a few hundred kHz in air. For example, a cube-shaped chip actuator with a side length of 2 mm (PL022 PICMA Chip Actuator, Physik Instrumente GmbH & Co. KG, Karlsruhe, Germany) has an unloaded resonant frequency of 300 kHz. An actuation bandwidth of 30 kHz was demonstrated with this actuator coupled to a cantilever holder [18]. Higher bandwidth is feasible with an optimized holder design. Nevertheless, the response time of an

* Corresponding author. Tel.: +90 212 359 6895.
E-mail addresses: hamdi.torun@boun.edu.tr, htorun@gmail.com (H. Torun).

0304-3991/$ - see front matter © 2012 Elsevier B.V. All rights reserved.
http://dx.doi.org/10.1016/j.ultramic.2012.07.023

AFM actuator is proportional to the ratio of its mechanical quality (Q) factor to its resonant frequency [19]. High Q-factor inherent to a stack piezo actuator can be compensated for reduced response time by controlling Q-factor electronically. This method has been implemented successfully using feedback loops [20–22]. In addition, alternative actuation technologies have been developed to reduce the response time of AFM cantilevers. For example, a response time of 90 μs is demonstrated using a novel method of actuating a force-sensing cantilever with a photothermally-actuated cantilever [23].

The purpose of this study is to describe and demonstrate a method using micromachined membrane-based electrostatic actuators for improved force-clamp experiments. These membrane actuators replace piezo actuators while the displacement of the force-sensing cantilever is measured using the optical lever detection mechanism of a conventional AFM system. Previously, we have used versions of these devices for molecular force spectroscopy measurements [24], fast molecular pulling experiments [25], and biomolecular force detection [26], but the actuator was not used in a closed loop for force clamp measurements. There are several advantages of the membrane type actuators. The diameter of a typical actuator membrane is 100–300 μm. The foot-print and the moving area of a typical device are much smaller than those of a piezo actuator commonly used in AFM setups. Thus the effective mass of the actuator is reduced significantly. The membranes can also be designed relatively stiff to achieve high speeds. For example, membranes made of silicon nitride/oxide have resonant frequencies of a few hundred kHz [24] in fluid. Moreover, membrane actuators have been shown to reduce the hydrodynamic drag forces experienced by the cantilevers thanks to their reduced area when compared to a piezo actuator [25]. Another advantage of the architecture of membrane actuators is that it is scalable for an array formation owing to microfabrication technology. It is feasible to use an array of membranes to precisely control and actuate an array of cantilevers.

In this paper we demonstrate a force-clamp setup employing the membrane actuators especially for biomolecular life-time experiments. We describe the operation of membrane actuators and present detailed characterization work. We also explain the control of actuators in a feedback loop. The experimental characterization results are presented along with initial biological experiments with the force-clamp setup which involved interactions between a biomolecular pair to demonstrate the feasibility of the method.

2. Experimental setup and device characterization

We fabricate electrostatic actuators using a 7-mask process with Parylene structural membrane on top of a silicon substrate. The electrodes are buried in the dielectric membrane to electrically isolate them from the fluid medium. The backside of the membrane was etched to reduce the damping effect and allow faster actuation rates. The details of the microfabrication process are explained elsewhere [26]. An illustration of the membrane structure with labeled parts is shown in Fig. 1a and the micrograph of a fabricated device is shown in Fig. 1b.

Stable displacement range of a parallel-plate electrostatic actuator is one-third of the initial gap height between its electrodes. Therefore, this range can be extended by simply increasing the gap height. However, this also will increase the voltage requirement for the operation. In addition, increasing gap height will introduce fabrication complexity. On the other hand, it is also possible to extend the stable displacement range of electrostatic actuators by simply segmenting the electrodes without a need for increased gap heights. This method was introduced to increase the range of a tunable diffraction grating device [27].

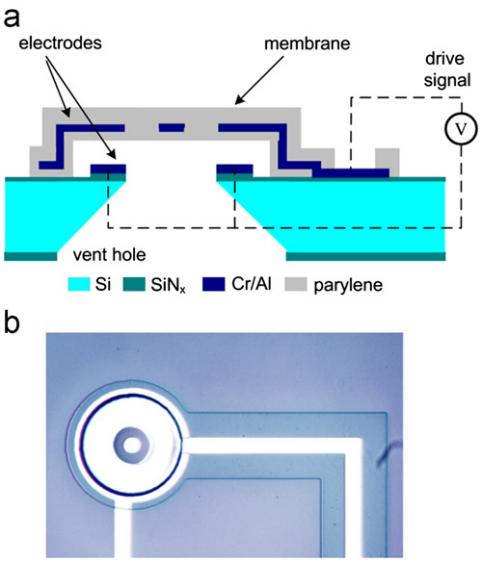

Fig. 1. (a) Schematic of a membrane actuator. (b) Micrograph of a fabricated membrane with a diameter of 300 μm.

We use segmented-electrode actuation method by patterning both bottom and top electrodes of actuator as shown in Fig. 1. For experimental characterization, the displacement range provided by a 150 μm diameter membrane was measured. Deflection of the membrane was measured by engaging an AFM cantilever at the center of the membrane. AFM cantilever monitored the displacement of the membrane as the voltage bias between the electrodes was increased. The spring constant of the membrane was 200 N/m and that of the cantilever was 0.01 N/m. Since the membrane was much stiffer than the cantilever, the loading of the cantilever on the membrane due to the engaged cantilever was insignificant. Fig. 2 shows that the membrane can be displaced more than 1.8 μm before it collapses to the substrate. The whole range requires less than 200 V-bias, which is comparable to the requirements of bulk piezo actuators commonly used in commercial AFM systems. The initial gap height was 2.5 μm, and a simple parallel plate electrostatic actuator with this gap would provide a range of 0.83 μm before collapse. The electrostatic actuation with side electrodes increased the range of a simple parallel-plate electrostatic actuator by more than 100%.

Within the full actuation range, the membrane is fast and the speed of actuation is limited only by the membrane dynamics. The resonant frequency of Parylene membranes in fluid is a few tens of kHz and within this bandwidth the responsivity is constant [26]. The calculated in-fluid resonance frequency of the particular membrane used in the experiments is 37 kHz. The resonant frequency of the membrane actuator can be increased above 100 kHz using silicon nitride/oxide membrane materials [24].

Electrostatic actuators are inherently non-linear actuators. However, when used to actuate AFM cantilevers for certain applications such as dynamic force spectroscopy, it is desirable to linearize the actuator. For linear operation, we drive the actuator by inputting computer generated signals based on a calibration routine. Fig. 2a is an example of a calibration curve with a fitted 3rd order polynomial function. For a desired membrane actuation, the corresponding voltage waveform is generated by a small routine written in LabVIEW 8.5 (National Instruments Corp.). A sample trace shown in Fig. 2b exhibits the linearity of the actuation method. Linear functions were fitted to the ramp-up and ramp-down sections of the graph. Adjusted-R^2 values for the lines were found as 0.99408 and 0.99407. So, an AFM cantilever can be actuated linearly by using a membrane

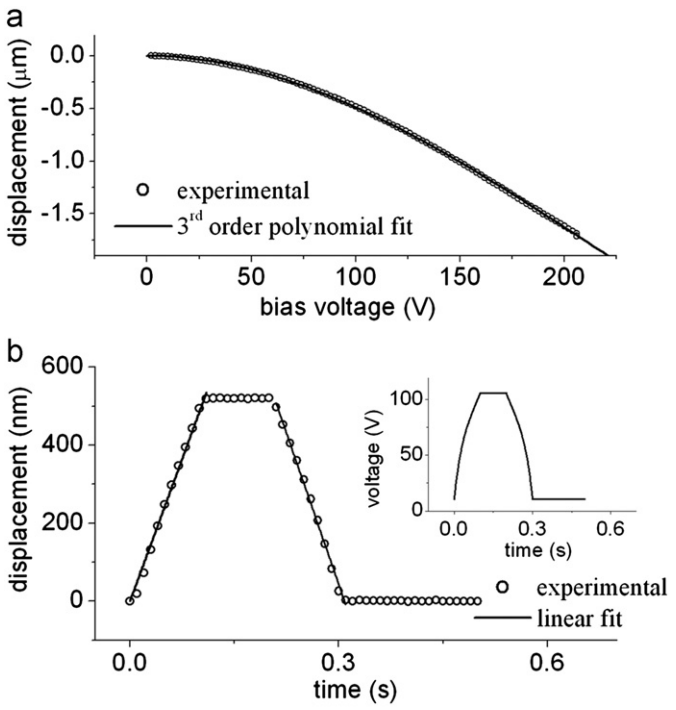

Fig. 2. (a) Displacement of a 150 μm diameter membrane actuator as a function of bias voltage. (b) A sample trace for the programmed actuation exhibiting the linearity of the actuator. Inset to graph shows the trace of applied voltage.

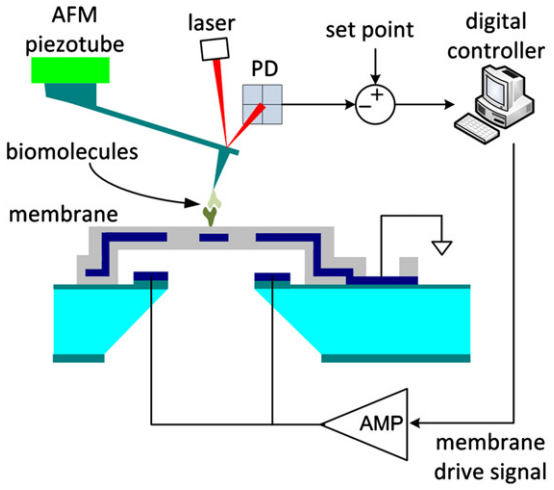

Fig. 3. Schematic of the experimental setup for biomolecular force-clamp experiments using electrostatic membrane actuators.

actuator with this routine. For the sake of completeness, the trace of applied voltage is shown in the inset to the graph. Fig. 2b is also helpful for the experimental determination for the accuracy of the actuator. Deviation of the cantilever position was within 0.8 nm when the membrane was kept still. We would like to note that this figure also includes effects of the readout noise and the drift in the system.

We implemented a digital controller for force-clamp experiments using LabVIEW 8.5 environment. The force-clamp setup is schematically shown in Fig. 3. In this setup, we fixed a membrane actuator on top of the sample stage of a commercial AFM system (Dimension 3100, Veeco Instruments). The force on the cantilever is kept constant at the user defined set point by the feedback loop that controls the membrane actuator. Here, displacement of the cantilever is acquired using a 16-bit data acquisition card (NI PCI 6229, National Instruments Corp.). This signal is compared with the set point and the error signal is fed to the controller. The controller generates the necessary compensation drive signal based on the membrane calibration. We have the flexibility to modify the controller and the set point during the operation with this method. Finally, the drive signal is then amplified and fed to the electrostatic actuator. We use a single-channel commercial amplifier: E-507 Amplifier Module (HVPZT, Physik Instrumente).

An important issue in the force-clamp setup is the uncertainty (noise and drift) in the AFM readout introduced by the membrane actuator. To characterize the additional uncertainty, we obtained the noise spectra of a 320 μm long, triangular-shaped cantilever made of silicon nitride for different cases using a dynamic signal analyzer (SR785, Stanford Research Systems). Displacement noise spectrum of this cantilever (MLCT-C, $k_{nominal}$=0.01 N/m, Veeco Probes) that is commonly used for biological applications is shown in Fig. 4. A simple harmonic oscillator (SHO) model fitted to the spectrum is also shown as a reference. Then we engaged this cantilever on a flat hard surface and obtained the noise spectrum again. The force on the cantilever was about 250 pN and the displacement spectrum is shown in Fig. 4. The shift in resonant peak and lower values of displacement around resonance is expected due to the stiffening of the cantilever. However, there are additional peaks introduced into the spectrum. We think this is due to the stage vibration. Finally we engaged the cantilever on a 200 μm diameter membrane actuator and clamped the force on the cantilever at about 250 pN. Fig. 4 shows the obtained spectrum. First observation is that the force-clamped cantilever exhibits a very similar spectrum with that of the cantilever engaged on a surface. That suggests that the force-clamping method described here does not introduce a substantial uncertainty. Yet, the displacement noise is slightly higher for the force-clamped cantilever. One contributing factor can be a shift on the cantilever force for the cantilever-on-surface case. We initially set it to 250 pN but since this case is open-loop, we did not have any precise control on the set force.

We characterized the force-clamp setup as shown in Fig. 5. We engaged a same type cantilever on another 200 μm diameter membrane and clamped the force on the cantilever at ~9 nN. Fig. 5a shows the time traces of the membrane operation and force deviation during the experiment. We disturbed the system using the piezo actuator three times by inputting external steps. The membrane actuator responded so that the clamp force stayed the same. The small indentations visible on the force trace

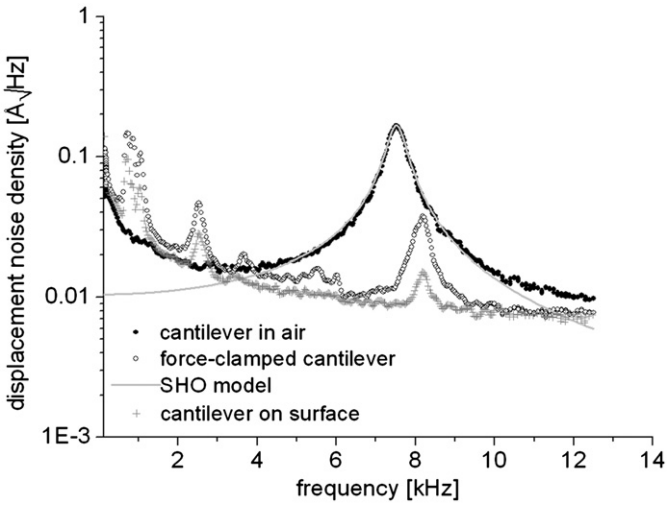

Fig. 4. Displacement noise spectrum of a cantilever (MLCT-C, $k_{nominal}$=0.01 N/m, Veeco Instruments) obtained for different cases.

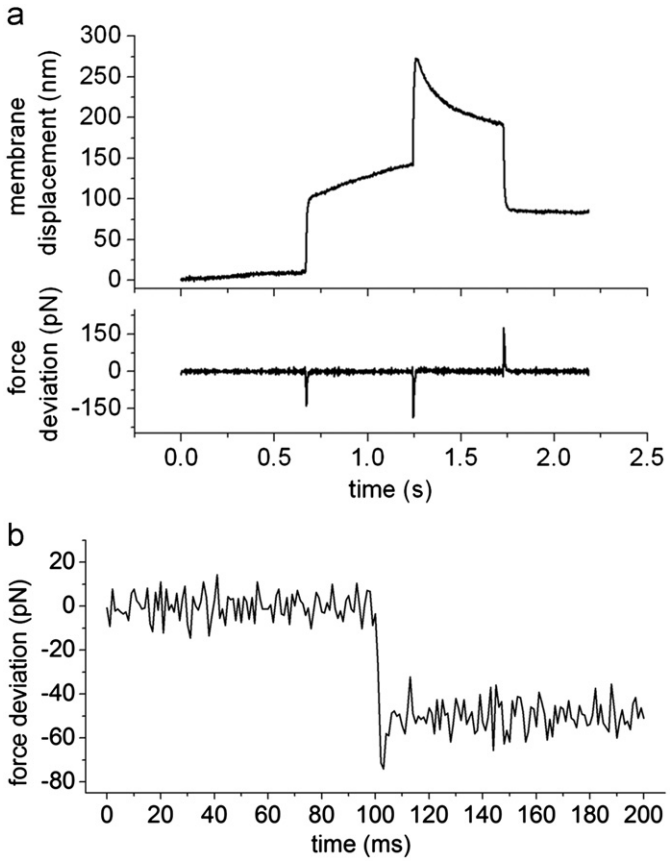

Fig. 5. (a) Sample force and displacement traces showing the operation of the force-clamp setup. The cantilever was disturbed by stepping the AFM piezo actuator. The membrane actuator responded to keep the set point constant. The small indentations on the force trace show the time instances of the steps. (b) A sample force trace showing the settling of the system from one clamp force to another one. The set point was decreased by about 50 pN during the operation and the membrane actuator settled in ~5 ms.

correspond to the time instances of the disturbances. Here, the membrane was able to keep set point for the piezo movement in both directions. One observation is that even when there is no disturbance, the membrane actuator moved to keep the force constant. This result indicates drift and mechanical instability in the system. Even when there is drift, the compensation is effective. So the system is suitable to measure life-time of a biomolecular pair when the bond is stressed at a fixed force.

For the characterization of settling time, we changed the set point while the system was running as shown in Fig. 5b. Initially the cantilever was clamped at ~300 pN and the clamped force was decreased by 50 pN at time ~0.1 s. The membrane actuator responded and it settled to its updated level in about 5 ms. This figure is comparable to that of AFM force-clamp setups employing piezo actuators [15,16]. We note that the settling time for our current setup is limited with the bandwidth of the amplifier we use. The 3 dB bandwidth of the amplifier unit for open load is 2 kHz (E-507 Amplifier Module (HVPZT, Physik Instrumente)). Since the feedback controller and the membrane actuator are much faster than the amplifier, it is possible to reduce the settling time considerably. The fundamental limit comes from the actuator itself and using stiffer nitride membranes, an actuation bandwidth of 400 kHz has been demonstrated [24]. With a quality factor (Q) of 5, the settling time (τ) of the actuator is less than 40 μs ($\tau = Q/\pi f_0$ [28]). So, this technology would be suitable for applications requiring fast force-clamp operation. Unlike photothermal actuators [29], this method does not require additional laser and optics for actuation and is relatively easy to operate.

3. Biological test system and experimental results

We used the force-clamp setup to measure biomolecular bond life-times. For the initial experiment, we probed the interactions between human IgG and anti-human IgG obtained from Sigma-Aldrich (St. Louis, MO). Prior to the force-clamp experiments we have performed constant-speed molecular pulling experiments to characterize biomolecular interactions. For this experiment, we used a 0.01 N/m stiff cantilever (MLCT-C, Veeco Probes) and the piezotube actuator of the AFM system (see Fig. 6a). The functionalization protocol included incubation of a hard substrate with 20 μl of anti-human IgG (10 μg/ml) for about 15 min at room temperature. Then the substrate was soaked with 1% BSA DPBS (from Sigma-Aldrich). The cantilever was incubated with 10 μl of human IgG (10 μg/ml) for about 15 min again at room temperature. We performed molecular pulling experiments by repeatedly moving a functionalized cantilever in and out of contact with a functionalized surface at different speeds. We gathered a total of ~1200 force curves to complete the experiment. We analyzed the results of pulling experiments to extract the so called Bell parameters: k^0_{off} and x_β, the off-rate at the absence of force and the barrier width, respectively using a recently introduced method [30]. Fig. 6b shows the force dependent off-rate plotted as a function of the force bin width. For a fixed force applied (F) on the bond, the thermal force (F_β) and the off-rate (k_{off}) is fixed and given as:

$$F_\beta = \frac{k_B T}{x_\beta}$$
$$k_{off} = k^0_{off} \exp\left(\frac{F}{F_\beta}\right) \quad (1)$$

Based on an exponential fit to the experimental data, k^0_{off} and x_β values were determined as 0.0055 s^{-1} and 0.41 nm, respectively. Fig. 6c shows a typical force curve when we recorded no binding/unbinding event among the collected force curves. On the other hand, Fig. 6d shows a recorded unbinding force of 38 pN for an experimentally measured pulling speed of 810 nm/s.

Next, we probed the interactions between the same pair of biomolecules using the force-clamp setup. We coupled another 0.01 N/m stiff cantilever with a 200 μm diameter membrane actuator with a stiffness of 150 N/m. We functionalized the membrane following the same steps we took for the hard substrate. We initiated the experiments with bringing the AFM cantilever in contact with the membrane that was already biased. After the point of contact, the controller carried out the operation. In the case of a bond formation, the membrane was first moved away from the cantilever so that the biomolecules were stretched with a user-defined set point force. Then this level was kept constant by updating membrane position until the point of unbinding. Unbinding event occurs when the molecular bond ruptures. At the point of rupture, the cantilever snaps back to its rest position and the controller stops its operation. In this experiment, we measured the elapsed time from the point of stretching to the point of rupture as life-time. Fig. 7a and b shows the measured life-times when the clamp force was set at 50 pN. These force traces suggest the life-time values of 1.08 s and 0.98 s.

We compared the life-time values obtained using force-clamp setup with the results of constant-speed molecular pulling experiments. We ran simple Monte-Carlo (MC) simulations to predict lifetime spectrum for a specified clamping force.

MC simulations comprise of a recursive comparison of instantaneous unbinding probability for time step ΔT with a random number

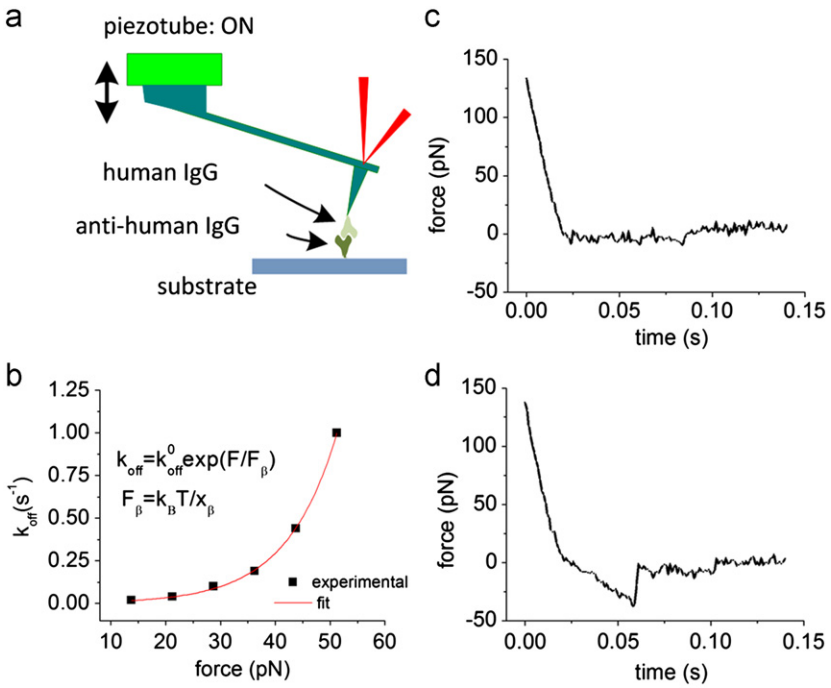

Fig. 6. (a) Schematics of the setup for constant-speed molecular pulling experiments to characterize human IgG and anti-human IgG molecular interactions. (b) Extraction of Bell parameters by fitting an exponential curve to the variation of off-rate as a function of force bin widths. This method is explained in detail elsewhere [30] (c) A typical force curve when no binding/unbinding event was recorded. (d) A typical force curve showing a recorded unbinding force of 38 pN for a pulling speed of 810 nm/s.

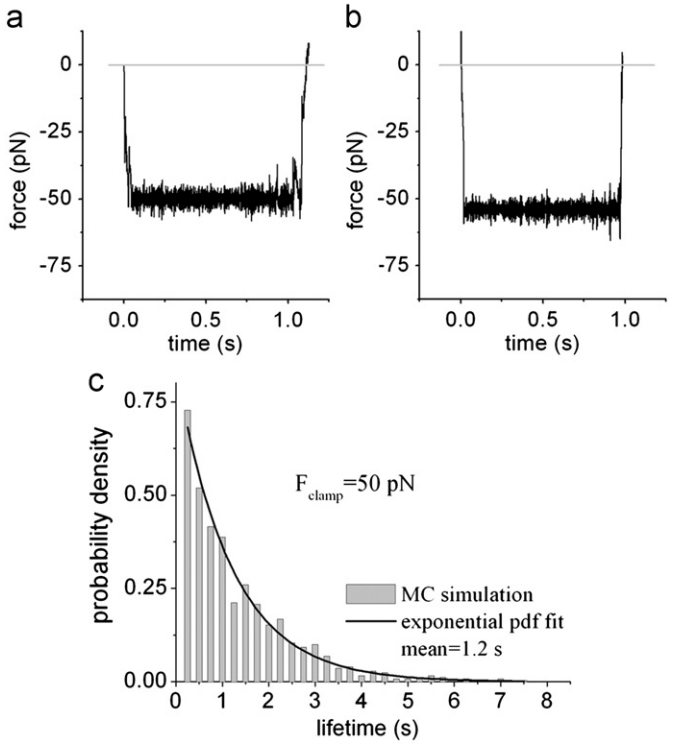

Fig. 7. (a and b) Sample force traces showing life-times for human IgG and anti-human IgG molecular pairs. The membrane actuator was controlled so that the force on the molecular bond was kept constant at 50 pN till the point of rupture. (c) Monte Carlo simulations showing the probability density function for the life-time when the bond is loaded with a clamp force of 50 pN. The mean of the distribution is in good agreement with the experimental results.

between 0 and 1. Instantaneous unbinding probability is given in Eq. (2) and if it is larger than the random number, bond is assumed broken. If not, time is stepped up until the bond gets broken. The time when the bond is broken is considered as the lifetime.

$$P_{rupture} = 1-\exp(-k_{off}\Delta T) \quad (2)$$

Fig. 7c shows the distribution of life-times when MC simulation was run for a clamping force of 50 pN. An exponential distribution function can be fitted to the life-time distribution. The mean value for the fitted probability density function is 1.24 s. This value independently validates the findings of the force-clamp experiments.

Distance recording is not necessary for the presented biological experiment where measurement of bond life-times is adequate. However, the capability of distance recording is needed for a variety of different experiments such as protein folding/unfolding. We would like to note that the presented force-clamp setup is suitable for independent force and distance measurements. The drive signal fed to the calibrated membrane actuator is used to monitor the displacement. The drive signal is an accurate measure for displacement for calibrated membranes as described in Fig. 2. Moreover, independent displacement measurement with picometer resolution is possible using an optical readout mechanism described elsewhere [26]. Fig. 8 shows the simultaneously captured force and membrane displacement data obtained by the explained force-clamp experiment. Here we set the force between the biomolecules at 80 pN while the membrane kept the set force constant till the time of rupture at $t=0.38$ s. For this example, the change in membrane position can be considered as a measure for the drift and mechanical instability associated with the current setup. Obviously, drift and stability control is very important for the experiments in need of accurate distance measurement.

4. Conclusion

In this paper we demonstrated a force-clamp setup employing micromachined membrane-based electrostatic actuators. The displacement range of the actuator is defined by the gap height between its electrodes. The current devices provide a displacement range of $\sim$1.8 μm with a reasonable voltage requirement. Parylene

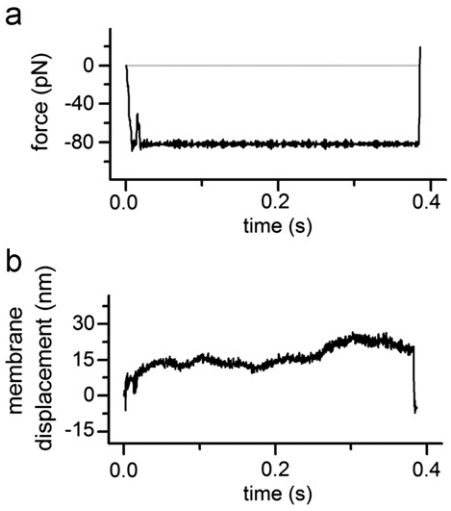

Fig. 8. Example force and membrane displacement data simultaneously captured during the biomolecular force-clamp experiment. The force between the biomolecules was set at 80 pN while the membrane kept the set force constant till the time of rupture at $t=0.38$ s.

membranes on silicon can be actuated with a bandwidth of a few tens of kHz in fluid. The nitride membranes on quartz are an order of magnitude faster. Both types of membranes may allow faster operation when compared with traditional piezo actuators. In addition to fast operation, cantilevers actuated by membranes are exposed to smaller hydrodynamic drag force due to the reduced actuation area [25]. We envision fast actuation capability with reduced drag forces using these membrane actuators. In addition, we aim to implement an array of micromachined membrane actuators to operate with an array of cantilevers. We use a software-based controller in our force-clamp setup. This is a flexible controller and can easily be modified. We can also update controller parameters during its operation. We characterized our setup in terms of response specifications. The clamp operation of the membrane does not introduce significant uncertainty on the cantilever readout. In a typical experiment, we found an uncertainty of 0.8 nm including system noise and drift. Transient response of the setup is currently limited by the amplifier we use and the settling time for the setup is $\sim$5 ms. This figure can be improved with a faster amplifier.

Finally, we performed biomolecular life-time measurements using this method as a feasibility work. Using the force-clamp setup, we stretched the molecular bonds between human IgG and anti-human IgG molecules. The controller kept the stretching force constant by updating the membrane position until we observed rupture events. We also verified the life-time values with molecular constant-speed pulling experiments which are in good agreement with simulations. These initial experiments indicate that this system architecture is suitable for various biomolecular mechanics measurements and it can be further improved as discussed here.

Acknowledgments

We would like to thank Dr. Fang Kong for his help in our experiments. This work was funded by the NIH (Grant No. R01 AI060799).

References

[1] J. Helenius, C.-P. Heisenberg, H.E. Gaub, D.J. Muller, Single-cell force spectroscopy, Journal of Cell Science 121 (2008) 1785–1791.
[2] X. Zhang, E.P. Wojcikiewicz, V.T. Moy, Dynamic adhesion of t lymphocytes to endothelial cells revealed by atomic force microscopy, Experimental Biology and Medicine 231 (2006) 1306–1312.
[3] B.T. Marshall, M. Long, J.W. Piper, T. Yago, R.P. McEver, C. Zhu, Direct observation of catch bonds involving cell-adhesion molecules, Nature 423 (2003) 190–193.
[4] G. Neuert, C. Albrecht, E. Pamir, H.E. Gaub, Dynamic force spectroscopy of the digoxigenin-antibody complex, FEBS Letters 580 (2006) 505–509.
[5] F. Schwesinger, R. Ros, T. Strunz, D. Anselmetti, H.-J. Guntherodt, A. Honegger, L. Jermutus, L. Tiefenauer, A. Pluckthun, Unbinding forces of single antibody–antigen complexes correlate with their thermal dissociation rates, Proceedings of the National Academy of Sciences of the United States of America 97 (2000) 9972–9977.
[6] J.M. Fernandez, H. Li, Force-clamp spectroscopy monitors the folding trajectory of a single protein, Science 303 (2004) 1674–1678.
[7] M. Schlierf, H. Li, J.M. Fernandez, The unfolding kinetics of ubiquitin captured with single-molecule force-clamp techniques, Proceedings of the National Academy of Sciences of the United States of America 101 (2004) 7299–7304.
[8] M. Rief, H. Grubmuller, Force spectroscopy of single biomolecules, ChemPhysChem 3 (2002) 255–261.
[9] A.F. Oberhauser, P.K. Hansma, M. Carrion-Vazquez, J.M. Fernandez, Stepwise unfolding of titin under force-clamp atomic force microscopy, Proceedings of the National Academy of Sciences 98 (2001) 468–472.
[10] H. Clausen-Schaumann, M. Seitz, R. Krautbauer, H.E. Gaub, Force spectroscopy with single bio-molecules, Current Opinion in Chemical Biology 4 (2000) 524–530.
[11] E. Evans, K. Ritchie, Dynamic strength of molecular adhesion bonds, Biophysical Journal 72 (1997) 1541–1555.
[12] E. Evans, K. Ritchie, Strength of a weak bond connecting flexible polymer chains, Biophysical Journal 76 (1999) 2439–2447.
[13] F. Kong, A.J. Garcia, A.P. Mould, M.J. Humphries, C. Zhu, Demonstration of catch bonds between an integrin and its ligand, Journal of Cell Biology 185 (2009) 1275–1284.
[14] M. Favre, S.K. Sekatskii, G. Dietler, Single-molecule avidin–biotin association reaction studied by force-clamp spectroscopy, Ultramicroscopy 108 (2008) 1135–1139.
[15] S. Garcia-Manyes, L. Dougan, C. Badilla, J. Bruji, J. Fernández, Direct observation of an ensemble of stable collapsed states in the mechanical folding of ubiquitin, Proceedings of the National Academy of Sciences of the United States of America 106 (2009) 10534–10539.
[16] C. Bippes, H. Janovjak, A. Kedrov, D. Muller, Digital force-feedback for protein unfolding experiments using atomic force microscopy, Nanotechnology 18 (2007) 044022–044028.
[17] D. Materassi, P. Baschieri, B. Tiribilli, G. Zuccheri, B. Samorì, An open source/real-time atomic force microscope architecture to perform customizable force spectroscopy experiments, Review of Scientific Instruments 80 (2009) 084301–084306.
[18] H. Torun, D. Torello, F.L. Degertekin, Note: Seesaw actuation of atomic force microscope probes for improved imaging bandwidth and displacement range, Review of Scientific Instruments 82 (2011) 086104–086103.
[19] T. Ando, T. Uchihashi, N. Kodera, D. Yamamoto, A. Miyagi, M. Taniguchi, H. Yamashita, High-speed AFM and nano-visualization of biomolecular processes, Pflügers Archiv: European Journal of Physiology 456 (2008) 211–225.
[20] A.D.L. Humphris, J. Tamayo, M.J. Miles, Active quality factor control in liquids for force spectroscopy, Langmuir 16 (2000) 7891–7894.
[21] T. Sulchek, R. Hsieh, J.D. Adams, G.G. Yaralioglu, S.C. Minne, C.F. Quate, J.P. Cleveland, A. Atalar, D.M. Adderton, High-speed tapping mode imaging with active Q control for atomic force microscopy, Applied Physics Letters 76 (2000) 1473–1475.
[22] T. Uchihashi, N. Kodera, H. Itoh, H. Yamashita, T. Ando, Feed-forward compensation for high-speed atomic force microscopy imaging of biomolecules, Japanese Journal of Applied Physics 45 (2006) 1904–1908.
[23] S. Stahl, E. Puchner, H. Gaub, Photothermal cantilever actuation for fast single-molecule force spectroscopy, Review of Scientific Instruments 80 (2009) 073702–073707.
[24] H. Torun, J. Sutanto, K.K. Sarangapani, P. Joseph, F.L. Degertekin, C. Zhu, A micromachined membrane-based active probe for biomolecular mechanics measurement, Nanotechnology 18 (2007) 165303–165310.
[25] K. Sarangapani, H. Torun, O. Finkler, C. Zhu, L. Degertekin, Membrane-based actuation for high-speed single molecule force spectroscopy studies using AFM, European Biophysics Journal 39 (2010) 1219–1227.
[26] H. Torun, K.K. Sarangapani, F.L. Degertekin, Fabrication and characterization of micromachined active probes with polymer membranes for biomolecular force spectroscopy, Journal of Microelectromechanical Systems 19 (2010) 1021–1028.
[27] E.S. Hung, S.D. Senturia, Extending the travel range of analog-tuned electrostatic actuators, Journal of Microelectromechanical Systems 8 (1999) 497–505.
[28] N. Kodera, H. Yamashita, T. Ando, Active damping of the scanner for high-speed atomic force microscopy, Review of Scientific Instruments 76 (2005) 053708-053705.
[29] S.W. Stahl, E.M. Puchner, H.E. Gaub, Photothermal cantilever actuation for fast single-molecule force spectroscopy, Review of Scientific Instruments 80 (2009) 073702–073706.
[30] M.J. Serpe, F.R. Kersey, J.R. Whitehead, S.M. Wilson, R.L. Clark, S.L. Craig, A simple and practical spreadsheet-based method to extract single-molecule dissociation kinetics from variable loading-rate force spectroscopy data, Journal of Physical Chemistry C 112 (2008) 19163–19167.